New Strategies for European Remote Sensing, Oluić (ed.)

A new rigorous model for the orthorectification of synchronous and asynchronous high resolution imagery

V. Baiocchi, M. Crespi, L. De Vendictis & F. Giannone
DITS - Geodesy and Geomatics, University of Rome "La Sapienza", via Eudossiana 18, 00184 Rome, Italy

Keywords: high resolution imagery, orthorectification, rigorous model, software

ABSTRACT: This paper proposes a new rigorous model for the orthorectification of high resolution imagery. Firstly, the model was developed and tested in the most general situation, that is considering the asynchronous EROS A satellite; now it is under extension in order to be able to process imagery acquired by other high resolution synchronous sensors (IKONOS II, QuickBird, SPOT 5).
Therefore it is necessary to model the high geometric distortions by a rigorous photogrammetric approach that requires the viewing geometry reconstruction through the knowledge of the acquisition mode, sensor features and satellite position and attitude.
The model was implemented in a C++ software *SISAR* and some tests were carried out to evaluate the intrinsic precision and accuracy achievable by using different angle off-nadir imagery. Results were compared with the corresponding ones obtained by the model implemented in the commercial software *OrthoEngine* 9.0 (PCI Geomatica), the only rigorous model for EROS A imagery presently available.
The comparison shows good agreement on the whole between the software as regards precision and accuracy; nevertheless, the model implemented in *SISAR* exhibits more stable dependencies of precision and accuracy on the Ground Control Point (GCP) number.
A final specific concern was devoted to the impact of outliers in GCP coordinates: the behaviours of two rigorous models (*OrthoEngine* 9.0 and *SISAR*) were again analyzed and compared to the one attaining to the second order Rational Polynomial Function (RPF) model implemented in *OrthoEngine* 9.0. In agreement with well-known theoretical deductions, the rigorous models exhibited a good robustness, whilst the RPF model proved to be highly vulnerable and inadequate for cartographic applications.

1 INTRODUCTION

High resolution remote sensing offers two remarkable advantages in cartographic production compared to aerial photogrammetry: regular interval acquisitions, dependent uniquely on the revisit period of the satellite used; possibility of imagery acquisition on inaccessible territories or countries where the organization of photogrammetric flights may be critical (e.g.: developing countries) (Holland et al., 2002).

However, the real possibility of using high resolution images for cartography depends on several factors: sensor characteristics (geometric and radiometric resolution); types of products com-

mercialized by the companies managing the satellites; cost and time to obtain these products (Table 1); cost of commercial software for processing such products.

Table 1. Comparison among the basic products stemming from the available high resolution satellites

Satellite	Product	Resolution (m)	Correction	Price per km^2 (March 2004)	Minimum acquirable area (km^2)	Stereopairs availability
IKONOS II	Geo Ortho Kit	1.0	Radiometric and geometric	$ 21.50	100	yes
EROS A	Standard 1A	1.8	Radiometric	$ 8.30	Not available	yes
QuickBird	Basic Imagery	0.6	Radiometric	€ 17.60	272	no
SPOT 5	Level 1A	5.0	Radiometric	€ 7.10	400	yes

It is evident that a full scene acquired by IKONOS II or QuickBird costs far more than those acquired by the other two satellites; this is due to both the price per square km and the lower limit of the acquirable area; it is especially this last factor that causes the price of a full scene from QuickBird to be almost three times as much as one from IKONOS II. On the contrary, for the EROS A products there are no lower limits on the area that has to be acquired; furthermore, the image low costs, together with the availability of stereopairs and the speed with which the satellite managing company can provide the product (few weeks) make the study of this satellite highly interesting.

In order to use these images for cartography, their distortions have to be corrected by orthorectification procedures, which, at present, are based on two main methods: Rational Polynomial Functions (RPF) and rigorous model (Toutin, 2004).

With RPF, the link between image and ground coordinates is described by a mathematical relation that does not consider the geometrical-physical process in image generation (Di et al., 2002). On the contrary, the rigorous approach is mainly photogrammetric (collinearity equations) and considers the satellite position, the sensor attitude and characteristics, the atmospheric refraction, the terrain morphology (using a DEM) and an eventual final cartographic transformation.

The commercial softwares often use Toutin's rigorous model, originally developed for SPOT and later extended also for Landsat and satellites with synchronous imaging acquisition (IKONOS II, QuickBird, SPOT 5). On the other hand, at present (April 2004) only the last version (9.0) of the *OrthoEngine* software contains a further extension of Toutin's model, especially developed for EROS A; no other rigorous model for asynchronous imagery is presently available both on the commercial and on scientific side.

In this context, it seemed worthwhile to define and implement a new rigorous model, able to orthorectify both synchronous and asynchronous imagery and it was decided to start just from the most general problem attaining asynchronous EROS A imagery.

The contents of the paragraphs are briefly summarized: in §2 the model theoretical fundamentals are presented; in §3 the model parameters estimation strategy, implemented into the new software *SISAR*, is described; in §4 the results of tests on some EROS A images, together with the comparison to those obtained by *OrthoEngine* software, are discussed; in the end, conclusions and future prospects are outlined.

2 FUNDAMENTALS OF THE RIGOROUS MODEL

As mentioned above, the orthorectification rigorous model correctly considers the satellite position, the sensor attitude and characteristics, the atmospheric refraction, the terrain morphology (using a DEM) and an eventual final cartographic transformation (Toutin, 2004).

This approach requires the reconstruction of the orbital segment during the acquisition through the knowledge of orbital parameters, of the sensor attitude and of some information on viewing geometry (internal orientation parameters, for EROS A the Field Of View) (Table 2).

Table 2. External (position and attitude) and internal orientation parameters for EROS A

Keplerian orbit parameters	Sensor attitude angles	Internal orientation parameters
a, half of major axis e, eccentricity i, inclination Ω, right ascension of the ascending node M, mean anomaly ω, argument of the perigee	$\varphi=\varphi_0+a_0+a_1t+a_2t^2$ (roll) $\theta=\theta_0+b_0+b_1t+b_2t^2$ (pitch) $\psi=\psi_0+c_0+c_1t+c_2t^2$ (yaw)	Field Of View (FOV)

The approximate values of these parameters are derived from the information contained in the *pass-file*, which is an ancillary file supplied with the EROS A1 images; nevertheless they must be refined by an estimation process based on a suitable number of Ground Control Point (GCP), for which collinearity equations are written.

In order to relate the image to the ground coordinates (expressed in an ECEF reference frame, usually a realization of WGS84, e.g. ITRF2000) by the collinearity equations, a set of rotation matrices (for details see Crespi et al., 2003) involving the following coordinate systems have to be used:

- Sensor coordinate system (S) - the origin is positioned at the perspective center (satellite's center of mass), the x_S-axis points to the direction of satellite motion, z_S-axis is directed from the array towards the perspective center, while y_S-axis is parallel to the array of detectors, completing a right-handed system
- Satellite coordinate system (B) - the origin is positioned at the perspective center (satellite's center of mass) and the x_B, y_B e z_B axes coincide with the Orbital coordinate system (F) (see below) axes when the attitude angles (ϕ, θ, ψ) are zero. The R_{SB} *(Body-Sensor)* matrix gives the transformation between the B-system and the S-system. It considers the non-parallelism between the axes $(x, y, z)_S$ and $(x, y, z)_B$ and is constant within one scene for each particular sensor; the matrix elements are provided be the *pass-file* as *camera-matrix*
- Orbital coordinate system (F) - the origin is positioned at the satellite's center of mass, the x_F-axis is tangent to the orbit in the same direction of satellite motion, the z_F-axis is in the orbital plane like the x_F-axis and points in the direction of the satellite's center of mass, while y_F-axis completes a right-handed system. The R_{BF} *(Flight-Body)* matrix gives the transformation between the F-system and the B-system through the attitude angles (φ, θ, ψ) varying in time
- Earth Centered Inertial (ECI) coordinate system (I) - the origin is positioned at the Earth's center of mass, the X-axis points to the Vernal Equinox relative to a certain epoch (J2000 -1 January 2000, h 12.00), the Z-axis points to the celestial North Pole in the same epoch while the Y-axis completes a right-handed system. The R_{FI} *(Inertial-Flight)* matrix gives the transformation between the I-system and F-system; it is a function of the Keplerian orbital parameters and thus varies in time within each scene

Finally, it is well known that the transformation between the considered realization of WGS84 and the ECI coordinate system is driven by precession, nutation, polar motion and Earth rotation matrices (Kaula, 1966).

It is now possible to write the collinearity equations in an explicit form for a generic ground point

$$x_s = f\frac{R_1\left|X_{tI} - X_{SI}\right|}{R_3\left|X_{tI} - X_{SI}\right|} \qquad y_s = f\frac{R_2\left|X_{tI} - X_{SI}\right|}{R_3\left|X_{tI} - X_{SI}\right|} \tag{1}$$

where (x_s , y_s) are the image coordinates, f is the focal distance, R_1, R_2, R_3 are the rows of the total rotation matrix $R = R_{SB}\, R_{BF}\, R_{FI}$ and (X_{tI} , X_{SI}) are the ground point and the satellite position in ECI system.

Moreover, since the focal distance f (~ 3.5 m) is not known with adequate precision, it is necessary to use the ratios x_s/f and y_s/f, dependent on the FOV through the following relationships, accounting that EROS A acquisition array contains 7043 pixels:

$$\frac{x_S}{f} = tg\beta = tg[(J - int(J) - 0.5) \cdot FOV] \qquad \frac{y_S}{f} = -tg\alpha = -tg[(I - 3521) \cdot FOV] \tag{2}$$

where (I-column , J-row) are the image coordinates (in pixels), so that the collinarity equations become:

$$F_1 = \frac{R_1 |X_{tI} - X_{SI}|}{R_3 |X_{tI} - X_{SI}|} - tg\beta = 0 \Rightarrow R_1 |X_{tI} - X_{SI}| - tg\beta\, R_3 \, |X_{tI} - X_{SI}| = 0$$

$$F_2 = \frac{R_2 |X_{tI} - X_{SI}|}{R_3 |X_{tI} - X_{SI}|} + tg\alpha = 0 \Rightarrow R_2 |X_{tI} - X_{SI}| + tg\alpha\, R_3 \, |X_{tI} - X_{SI}| = 0 \tag{3}$$

3 PARAMETERS ESTIMATION

The collinarity equations (3) may be rewritten explicitly with respect to all the parameters of Table 2 accounting that R_1, R_2, R_3 and X_{SI} depend on time through both Keplerian orbit parameters and attitude angles. Nevertheless some additional remarks are needed in order to define the parameters estimation procedure.

First of all, since the orbital arc relative to one image acquisition is quite short (~1/300 of the orbit length), the eccentricity (e), the argument of perigee (ω), and the semi-major axis (a) cannot be estimated and have to be constrained to the approximate values provided in the *pass-file*. Therefore, only 3 orbital parameters (Ω: right ascension of the ascending node; i: orbit inclination; T_p: time of perigee passage), 9 coefficients of the 2nd order polynomials (a_0, a_1,..., c_2) expressing the attitude corrections and 1 internal orientation parameter (FOV) are corrected and 7 GCP are required at minimum. These corrections are estimated in the usual least-squares sense; as the collinarity equations (3) are not linear, they are linearized according to the observables (I,J), the GCP ECEF coordinates (X,Y,Z) and to the parameters themselves (Ω, i, T_p; a_0, a_1,..., c_2; FOV) (Teunissen, 2001).

Moreover, the collinarity equations hypothesize that ground point, image point and perspective center belong to the same straight line, neglecting the ground displacement due to atmospheric refraction, which may be relevant especially under large *off-nadir* (γ) acquisition angles (0.5 m at 10°, 7 m at 50°). Therefore, this effect must be evaluated during both the 13 parameter corrections estimation and the subsequent orthorectification procedure; the strategy adopted is described in (Noerdlinger, 1999).

Therefore, the estimation procedure is carried out in three steps:

1. Estimation of the corrections for the Keplerian orbit parameters (Ω, i, T_p) only through a single iteration, just to roughly improve the satellite position
2. Evaluation of the ground displacement due to atmospheric refraction at each GCP; the GCP coordinates are corrected in order to eliminate the refraction effect and a second estimation of the corrections for the Keplerian orbit parameters is performed
3. Estimation of the attitude correction coefficients (a_0, a_1,...c_2) and internal orientation parameter (FOV) correction in successive iterations (the iterative procedure is stopped when the variance of unit weight $\hat{\sigma}_0$ reaches a minimum)

Moreover, concerning the stochastic model, a simple diagonal cofactor matrix for observation (I,J) was assumed; as regards the a priori variance of unit weight σ_0, its value was set considering that collimation tests carried out independently by two operators showed that an accuracy of about half a pixel (~1 m) in image coordinates may be easily achieved.

At the end of the estimation process, the intrinsic precision of the model may be evaluated by the RMS of the GCP coordinate residuals, whilst the RMS of the Check Point (CP) coordinate residuals represents the external accuracy. It is well known that CP are known ground points not used in the parameter estimation process, but it has to be underlined that the atmospheric refraction has to be accounted for in this case too.

4 SOFTWARE *SISAR* IMPLEMENTATION AND TESTING

The described estimation and precision/accuracy procedure was implemented into the C++ software *SISAR*, consisting of about 3000 lines and 10 principal subroutines. This software was tested on real data and compared with the well-known *OrthoEngine* software, in order to evaluate the performances of the new proposed rigorous model.

4.1 *Intrinsic precision and external accuracy: comparison with OrthoEngine*

The experimentation was based on four type 1A EROS A images with nominal ground resolution of 1.8 m:

1. MBT1-e1009023 (Rome, Italy): Feb 2, 2001; γ start = 15.3°, γ = 16.4°; area 10x14 km
2. ITA1-e1038452 (Rome, Italy): Aug 14, 2001; γ start = 9.1°, γ = 9.4°; area 10x12 km
3. ITA1-e1090724 (Rome, Italy): Jul 22, 2002; γ start = 31.0°, γ = 40.1°; area 18x12
4. ITA1-e1077263 (Tirana, Albania): Apr 25, 2002; γ start = 6.6°, γ = 17.8°; area 12x12

On the Rome and Tirana images 56 and 29 (N_{tot}) well identifiable and almost uniformly distributed points were respectively chosen. They were surveyed with static or fast static procedure by a Trimble 5700 GPS receiver and their coordinates were estimated by Trimble Geomatic Office software with respect to available GPS permanent stations (MOSE at Rome Faculty of Engineering for Rome, OHRI at Ohrid-Macedonia for Tirana); finally, the ellipsoidal heights were transformed into orthometric applying geoid undulations by ITALGEO95 model for Rome and European Geoid EGG97 model for Tirana. The estimated horizontal and vertical accuracies were respectively 0.1-0.3 m for Rome and 0.3-0.6 m for Tirana, both suited for using the points as GCP and CP, accounting for the images nominal resolution (1.8 m).

With the aim to evaluate the intrinsic precision of the model and the external accuracy achievable from the pure geometric point of view, (not accounting for the photointerpretation uncertainty, which may be larger for some objects), some tests (Figures 2 and 3) were carried out increasing regularly the GCP number starting from 9, the minimum requested by *OrthoEngine* software in order to guarantee a minimum redundancy (1 GCP). Two rules were followed: in all the tests GCP are almost uniformly distributed; if a point is selected as GCP in a certain test, it remains as GCP in all the subsequent tests with larger GCP numbers.

Test results showed that precisions tend to a constant values when GCP number increases; for each image these values (generally different for North and East coordinate) were estimated by an iterative backward procedure:

1. Starting from the RMS of the GCP coordinate residuals related to the last three tests (e.g. tests with 56, 52 and 48 GCP for the images of Rome), the initial mean RMS value is computed
2. The RMS of the previous test (e.g. test with 44 GCP for the images of Rome) is added and the RMS mean is recomputed

3.1 If a 2σ Chebicev test does not evidences any outlier, an other iteration starts from step 2

3.2 Otherwise the procedure is stopped and the searched constant value is the mean RMS at previous iteration

This procedure leads to two by-products (Table 3):

- The minimum number of GCP above which precisions may be considered constant for North and East coordinate ($\overline{N}_N$, $\overline{N}_E$) and globally ($\overline{N} = \max(\overline{N}_N, \overline{N}_E)$)
- The achievable external accuracy, computed as the RMS of the coordinate residuals of all the points ($N_{tot} - \overline{N}$), used as CP, not included in the minimum number of GCP above which precisions may be considered constant; in this way, the accuracy is evaluated on the largest set of points for each image.

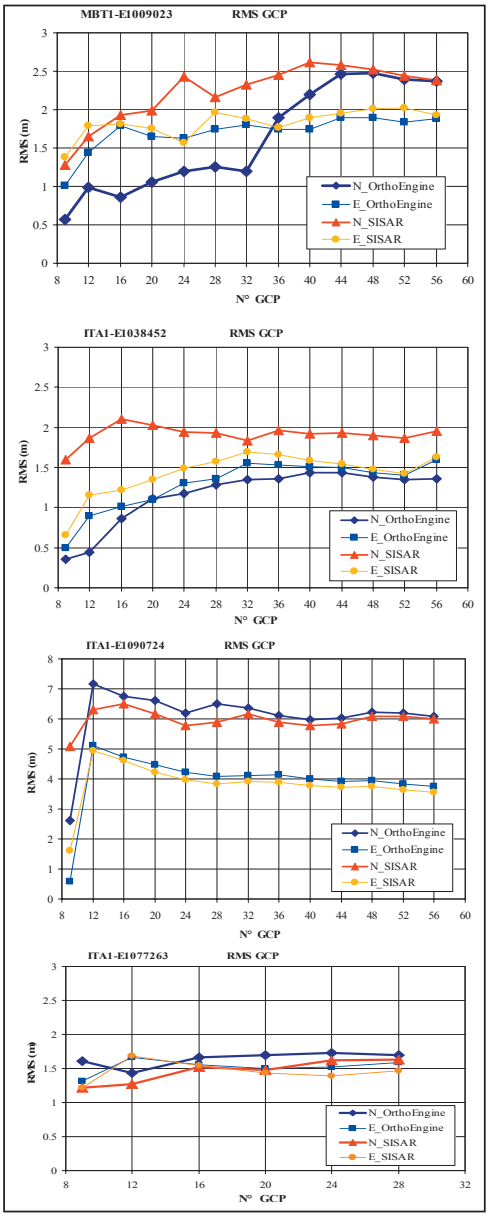

Figure 2. Intrinsic precisions vs. GCP number

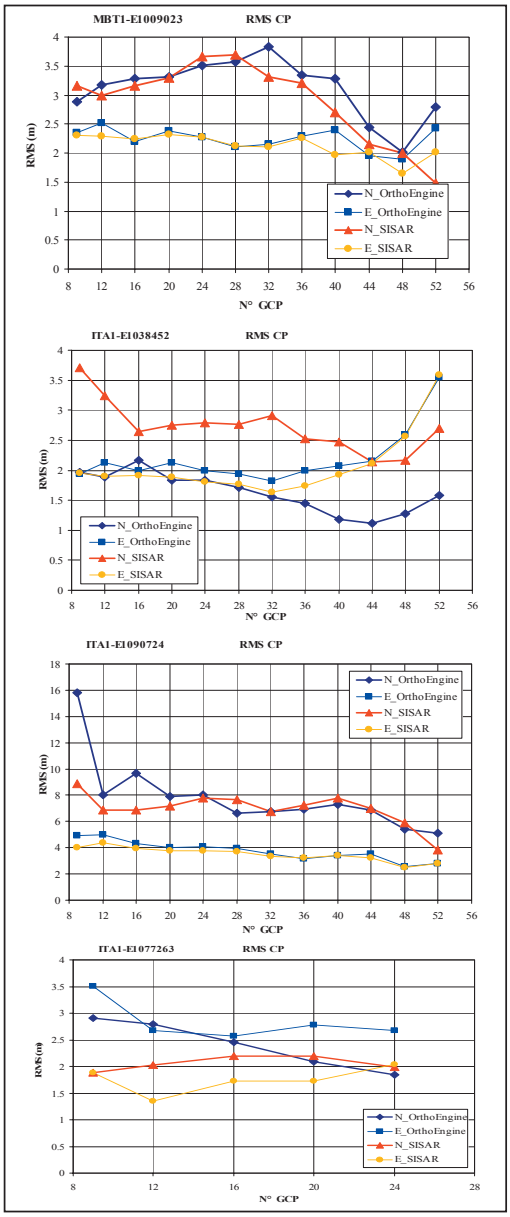

Figure 3. External accuracies vs. GCP number

Table 3. Estimated intrinsic precision and external accuracy for each image

Software	Intrinsic precision (residual RMS on GCP)					External accuracy (residual RMS on CP)		
	MBT1-E1009023		γ start 15.3		γ end 16.4			
	N (m)	E (m)	$\overline{N}_N$	$\overline{N}_E$	$\overline{N}$	$N_{tot} - \overline{N}$	N (m)	E (m)
SISAR	2.43	1.96	24	28	28	28	3.69	2.12
ORTHOENGINE	1.90	1.79	36	16	36	20	3.35	2.29
	ITA1-E1038452		γ start 9.1		γ end 9.4			
	N (m)	E (m)	$\overline{N}_N$	$\overline{N}_E$	$\overline{N}$	$N_{tot} - \overline{N}$	N (m)	E (m)
SISAR	2.03	1.35	20	20	20	36	2.76	1.77
ORTHOENGINE	1.28	1.31	28	24	28	28	1.84	2.12
	ITA1-E1090724		γ start 31.0		γ end 40.1			
	N (m)	E (m)	$\overline{N}_N$	$\overline{N}_E$	$\overline{N}$	$N_{tot} - \overline{N}$	N (m)	E (m)
SISAR	6.16	3.97	20	24	24	32	7.79	3.79
ORTHOENGINE	6.74	4.21	16	24	24	32	8.02	4.09
	ITA1-E1077263		γ start 6.6		γ end 17.8			
	N (m)	E (m)	$\overline{N}_N$	$\overline{N}_E$	$\overline{N}$	$N_{tot} - \overline{N}$	N (m)	E (m)
SISAR	1.22	1.22	9	9	9	19	1.89	1.88
ORTHOENGINE	1.61	1.32	9	9	9	19	2.91	3.51

On the basis of the test results some conclusions can be addressed:

- The minimum number of GCP $\overline{N}$ is quite variable in different images
- Precision cannot be estimated on the basis of a number of GCP smaller than $\overline{N}$, otherwise RMS of the GCP coordinate residuals results underestimated
- Accuracy cannot be estimated on the basis of a number of GCP smaller than $\overline{N}$, otherwise RMS of the CP coordinate residuals results overestimated
- *SISAR* and *OrthoEngine* behave similarly as regards precision and accuracy but *SISAR* seems more stable since the final precision value is reached with a less number of GCP ($\overline{N}$)

4.2 *Outlier effects: comparison with OrthoEngine rigorous and 2nd order RPF models*

It is well known that a fundamental advantage of rigorous models with respect to RPF models is their robustness in the presence of outliers. In order to test the effect of outliers on the new model, the positions of two points used as GCP for Rome images were modified, introducing outliers of 10 m on both coordinates, approximately 5 times the external accuracy obtained without outliers .The 2nd order RPF model requires at least 19 GCP; in order to guarantee a 20% redundancy 23 GCP were considered both for RPF and for rigorous model.

Both rigorous models are able to point out the four outliers by inspecting the normalized residuals (grey) and their accuracies are not affected by the outliers; otherwise, only some outlier may be detected with RPF model and its accuracy is extremely degraded by the outliers (Table 4).

5 CONCLUSIONS AND FUTURE PROSPECTS

In this work a new rigorous model for the orthorectification of satellite imagery is proposed. At present the model has been implemented into the software *SISAR* able to process EROS A asynchronous imagery and it was compared with *OrthoEngine*, the only commercially available software able to perform an analogous rigorous processing.

Results obtained on four images showed analogous performances both concerning intrinsic model precision, external accuracy and robustness against outliers, but *SISAR* seems more stable

since the final precision value is reached with a less number of GCP ($\overline{N}$). Of course further investigations on other images are needed to assess these preliminary results.

Future research prospects are oriented towards the extension to other high resolution synchronous sensors (IKONOS II, QuickBird, SPOT 5), the generation of the orthorectified imagery both in GRASS and in IDL environment, the DEM extraction from stereopairs and the aerial triangulation of synchronous and asynchronous high resolution satellite imagery blocks.

Table 4. Outliers effects on image ITA1-e1038452

Outliers 10 m	2nd ord. RPF model *O.Engine*				Rigorous model *OrthoEngine*				Rigorous model *SISAR*			
	w/o outliers		with outliers		w/o outliers		with outliers		w/o outliers		with outliers	
23 GCP	N(m)	E(m)	N(m)	E(m)	N(m)	E(m)	N(m)	E(m)	N(m)	E(m)	N(m)	E (m)
Accuracy	2.64	2.42	12.90	3.53	1.71	1.86	1.88	1.82	2.68	1.84	2.66	1.85
Norm.res. GCP 34	0.45	1.59	-3.88	-1.68	-0.66	1.71	-3.25	-2.36	0.05	1.75	-2.85	-2.24
Norm.res. GCP 53	0.43	-0.19	0.82	-0.08	1.28	1.36	-2.03	-2.78	0.61	1.35	-2.72	-2.62

ACKNOWLEDGEMENTS

Special thanks to Marola Corsetti, Francesca Lorenzon, Marco Mezzapesa, Giorgia Olivieri and Francesca Quattrone for their contributions to software development and testing and to IPT S.r.l. for having supplied the EROS A imagery.

This research was funded by the Italian Ministry for School University and Research in the frame of the National Research Relevant Project "L'automazione nei processi di acquisizione e gestione dei dati topo-cartografici a supporto delle iniziative dell'Intesa Stato-Regioni-Enti locali per i sistemi informativi geografici" (National chief Prof. Elio Falchi, Subproject chief. Prof. Mattia Crespi).

REFERENCES

Bar-Lev M., Shcherbina L. & Levin V. 2001. *Eros system - Satellite orbit and constellation design*. 22nd Asian Conference on Remote Sensing, 5-9 November, Singapore, vol. 2: 1153-1158

Chen L.C. & Teo T.A. 2001. *Orbit adjustment for Eros A high resolution satellite images*. 22nd Asian Conference on Remote Sensing, 5-9 November, Singapore, vol. 2: 1169 -1174

Chen L.C. & Teo T.A. 2002. *Rigorous generation of digital orthophotos from Eros A high resolution satellite images.* ISPRS, Commission IV, WG IV/7

Crespi M., Baiocchi V., De Vendictis L., Lorenzon F., Mezzapesa M. & Tius E. 2003. *A new method to orthorectify EROS A1 imagery.* Proc. of 2003 Tyrrhenian Int. Workshop on Remote Sensing, pp. 566-575

Di K., Ma R. & Li R. 2003. *Rational Functions and Potential for Rigorous Sensor Model Recovery* Photogrammetric Engineering and Remote Sensing 69 pp. 33-41

Holland D., Guilford B. & Murray K. 2002. *Oeepe-Project on Topographic Mapping from High Resolution Space Sensors* OEEPE, Official Publication No. 44

Jacobsen K. 2002. *Geometric aspects of the handling of space images* ISPRS, Comm. I, WG I/5, Denver

Kaula W. M. 1966. *Theory of Satellite Geodesy* Blaisdell Publishing Company

Noerdlinger P. D. 1999. *Atmospheric refraction effects in Earth remote sensing* ISPRS Journal of Photogrammetry & Remote Sensing 54 pp. 360–373

Teunissen P. J. G. 2001. *Adjustment theory* Series on Mathematical Geodesy and Positioning

Toutin T. 2004. *Geometric processing of remote sensing images: models, algorithms and methods (review paper)* in press on International Journal of Remote Sensing, 10 pp. 1893-1924

Westin T. 1990. *Precision Rectification of SPOT Imagery* Photogrammetric Engineering and Remote Sensing 56 pp.247-253

Westin T. & Forsgren J. *Orthorectification of Eros A images* www.imagesatintl.com